

DESIGN, FABRICATION, AND PERFORMANCE TESTS OF DIPOLE AND QUADRUPOLE MAGNETS FOR PAL-XFEL*

Hyung Suck Suh[#], Bongi Oh, Dong Eon Kim, Heung-Sik Kang, Hong-Gi Lee, In Soo Ko, Ki-Hyeon Park, Moo Hyun Cho, Sang-Bong Lee, Seong Hun Jeong, Young-Gyu Jung
PAL, Pohang, Republic of Korea

Abstract

PAL(Pohang Accelerator Laboratory)-XFEL is now being constructed in Pohang, Korea. This facility will consist of a 10 GeV linac and five undulator beamlines. As the first phase we will construct one hard X-ray and one soft X-ray beamlines which require 6 different families of dipole magnets, and 11 families of quadrupole magnets. We have designed these magnets with considering the efficient production and the proper power supplies. In this presentation, we describe the design features of the magnets, the manufacturing, and the thermal analysis with the test results.

INTRODUCTION

The PAL-XFEL is a 0.1-nm hard X-ray FEL project starting from 2011. Three hard X-ray and two soft X-ray branches are planned. As the first phase of this project, one hard X-ray (HX1) and one soft X-ray (SX1) which consist of 51 dipole and 208 quadrupole magnets will be constructed [1].

We have designed all magnets on our own by using OPERA and ANSYS codes [2, 3]. We tried to reduce the number of coil types and the number of the power supply types for the convenient production. Every magnet is designed to maintain the maximum temperature rise of coils below 20 K for about 120% of the rated currents. In the process of the design, it was helpful to parameterize the main figures of the magnets in a spread sheet for easy estimation by changing some parameter often. Now we are manufacturing them and testing the prototype magnets.

DIPOLE MAGNETS

The dipole magnets were classified into 6 kinds according to the pole gap, the effective magnetic length, and the maximum magnetic field. The results of the classification are listed in Table 1.

Dipole magnets have the same pole gaps of 30 mm except D6 of 15 mm for the self-seeding. D1, D2, and D4 have H-type core shape, and D3, D6, and D7 have C-type. All dipole magnets of D1~D6 for the bunch compressor, the chicane, and the self-seeding have the trim coils with 1% of the main field.

The pole profiles of magnets are optimized by the small bumps at the tip of the pole for the field uniformity. The requirements for the field uniformity are different from each magnet, e.g. in the case of H-type dipole magnet D1,

$\Delta B/B_0 < 1.0E-4$ for ± 17 mm, $\Delta B/B_0 < 5.0E-4$ for ± 41 mm in 3D calculation.

Table 1: The Families of Dipole Magnets (D5 was Replaced with D2)

Family	Magnetic length [m]	Max. field [T]	Qty	Position
D1	0.20	0.80	6	BC1
D2	0.70	1.00	18	BC2,BC3, BAS1
D3	1.50	1.30	11	BAS2,3,4
D4	0.17	0.30	4	Laser Heater
D6	0.30	0.485	4	Self seeding
D7	0.75	1.164	2	Tune-up dump

So the pole contour of D1 is made like Fig. 1 where the a-b line has a slight slope. The 2D/3D field uniformities of the calculation results are shown in Fig. 2.

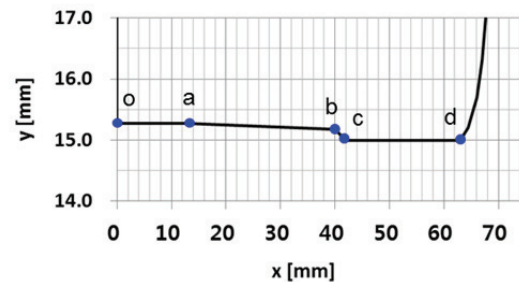


Figure 1: Pole contour of H-type dipole magnet D1.

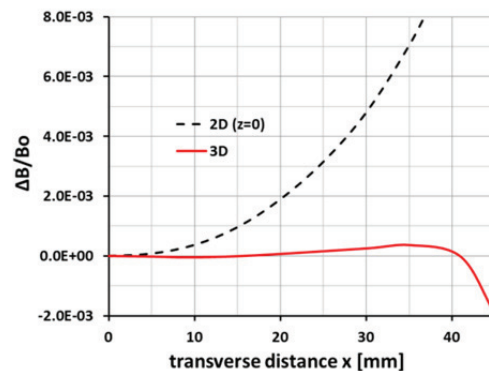


Figure 2: Calculated 2D/3D field uniformities of dipole magnet D1.

The laminated cores are used for the magnets D2 and D3 which quantities are more than 10 magnets, and the solid cores are used for the rest of the dipole magnets.

*Work supported by Ministry of Science, ICT and Future Planning of Korea, #suhhs@postech.ac.kr

We measured the magnetic field of D4 dipole magnet that has four coils per magnet for the space in the middle (see Fig. 3). The 3D results of the field uniformity satisfied the requirement that is less than 1.0E-4 within ±9 mm as shown Fig. 4. But now we are analysing the multipole components along the beam trajectory.

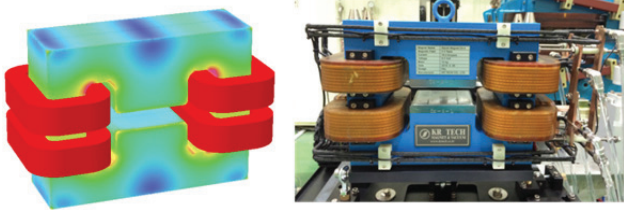


Figure 3: The FEM model and the prototype of dipole magnet D4.

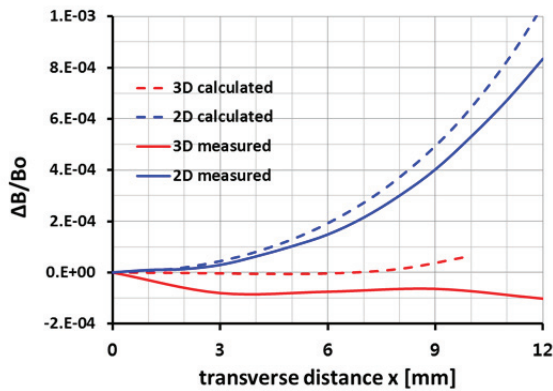


Figure 4: Field uniformity comparison of D4 magnet.

QUADRUPOLE MAGNETS

The quadrupole magnets are classified into 11 kinds according to the aperture diameter, the effective length, and the maximum field gradient. The results of the classification are listed in Table 2.

Table 2: The Families of Quadrupole Magnets

Family	Aperture diameter [mm]	Magnetic length [m]	Max. gradient [T/m]	Qty
Q1	30	0.065	15	18
Q2	30	0.13	25	60
Q3	30	0.18	25	18
Q4	44	0.20	25	7
Q5	22	0.40	35	14
Q6	16	0.13	40	31
Q7	80	0.50	18	3
Q8	22	0.25	30	19
Q9	16	0.08	32	18
Q10	44	0.50	25	4
Q11	44	0.10	10	16

There are the horizontal and vertical steering functions in some quadrupole magnets (Q1, Q2, Q3, Q6, and Q9) for the bunch compressors and the inter-undulator.

The multipole components were calculated by using an equation, the radial component: $B_r(r_0, \varphi) = \sum_n \{A_n \sin(n\varphi) + B_n \cos(n\varphi)\}$, where r_0 is the reference radius that is the good field radius. All magnets are optimized to have the relative multipole components less than 1.0E-4 in 3D calculations. Fig. 5 shows the half pole contour. In this figure the o-m line follows along an ideal hyperbola, the m-n is a straight line and an arc after n point. We could satisfy the multipole requirements by manipulating the position and the length of the straight section.

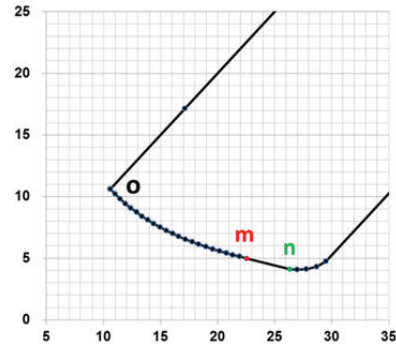


Figure 5: The half pole of quadrupole magnet.

The indirect cooling system (heat sink) for the quadrupole magnets (Q1, Q2, Q3, Q5, Q6, Q8, and Q9) was adopted. Fig. 7 shows the cross section of the conductor and the temperature distribution of quadrupole magnet Q2. We used the effective thermal conductivity: $1/k_{eff} = \sum v_i/k_i$ for the turn insulation and the ground insulation, where v_i is the volume fraction.

We made two kinds of prototype quadrupole magnet of Q2 and Q5, and measured the magnetic field with a hall probe and the temperature rise (see Fig. 6 and Table 3).

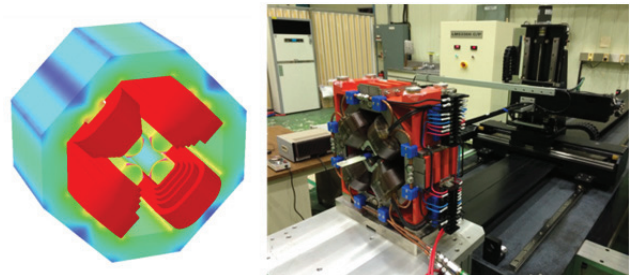


Figure 6: FEM model and field measurement scene of a quadrupole magnet.

Table 3: The Calculated and Measured Temperature Rise

Magnet	Calculated	Estimated (by resistance)	Measured
Q2	11	16	14
Q5	10	15	17

The relative deviation of the field gradient $\Delta B'/B'$ for Q2 was shown as 1.2E-3 within ±10mm on the mid-plane. We prepare the field clamp to shield the leakage field from quadrupole magnets. The field clamp of 1 mm

thickness can reduce the leakage field to less than 5 Gauss beyond this clamp. But this field clamps reduce the magnetic length by about 1% for Q2.

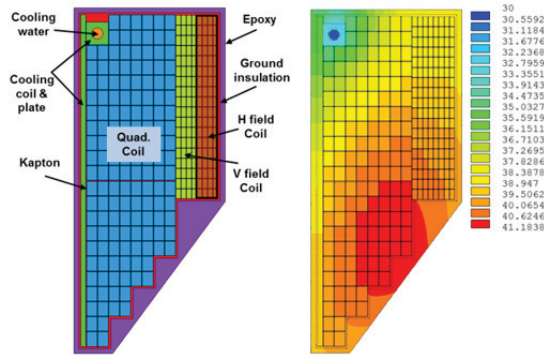


Figure 7: The conductor cross section and the temperature distribution of quadrupole magnet Q2 with a heat sink.

CORRECTOR MAGNETS

The dipole magnets and the quadrupole magnets for the chicanes and the beam analysing have the trim coils or the horizontal/vertical steering coils respectively. Beside these, we prepare the independent corrector magnets of 49 that are composed of 35 with iron core and 14 with air core. The other correctors with iron core have the heat sink system similar to Fig. 7 for the narrow space. The main parameters of the corrector magnets are shown in Table 4.

Table 4: The Main Parameters of Corrector Magnets

Corrector type	C1	C2	C3
Core	iron	iron	air
Cooling type	air	heat sink	air
Field integral [Gcm]	5000	5000	1000
Magnet length [mm]	295	144	200
Current density [A/mm ²]	1.1	2.6	0.9
Temperature rise [K]	16	12	18
Quantity	35	6	14

CONCLUSION

When we classified the magnets and determined the coil sizes, we should consider the connection condition of magnets in series or stand alone, the electrical properties of magnets, and the number of cooling circuit. If the number of cooling circuits is increased in order to reduce the temperature rise, then the magnets become more complicate with the risk of leakage [4].

We have designed almost all magnets, and are testing the prototype magnets now. The results of tests are not bad until now. But we have to modify magnets if it is necessary after analysing the magnetic field and the temperature rise.

REFERENCES

- [1] PAL-XFEL, Beam Optics and Parameter Design, Heung-Sik Kang, 2012.
- [2] Vector Fields Software, <http://www.cobham.com>
- [3] ANSYS, <http://www.ansys.com>
- [4] Jack T. Tanabe, "Iron Dominated Electromagnets", 2005, pp. 113-126.